FOUNDATION FAILURE OF NEW LISKEARD EMBANKMENT

Gerald P. Raymond, Queen's University, Kingston, Ontario

A case history of an embankment foundation failure in varved clay is presented. Stability analyses by total stress, partial total stress, effective stress, and finite elements have been obtained and are discussed. Attention is focused on the performance of the stiff crust, the selection of the soil properties, and the placement of the instrumentation.

•THE NORMAL METHOD of estimating the immediate bearing capacity of surface loads on saturated cohesive soils is to assume that the soil is a purely cohesive material with a unique strength. In special cases a slip circle analysis is performed. The theoretical solutions of the slip circle method for deposits with a uniform cohesive strength have been presented by Jakobson (9), and for soils whose strength increases linearly with depth extensions have been done by Odenstad (13), Nakase (11, 12), and Raymond (15). The method may also be extended to account for anisotropy and two-layered deposits. These methods are often referred to as total stress analyses. Unfortunately the major difficulties result not from the theoretical methods but from their application in terms of selecting representative soil strengths. In addition, where the loaded contact area is not rigid, a localized general failure may occur. A localized general failure has been defined by Raymond (15) as a general failure of part of the contact area and should not be confused with Terzaghi's (22) definition of local shear failure (Art 47) or the point at which the elastic limit is first exceeded (Art 138). Terzaghi's definition of local shear failure may be considered to be similar to that used by Gibson (7) for the end bearing capacity of a pile.

An alternative to the total stress analysis is the effective stress analysis. This method is of particular importance where stage construction techniques are employed and a gain in strength of the foundation material is relied on to complete the construction. The effective stress analysis normally used takes the form of a slip circle divided into slices. The slice method was first used by Felenius (5, 6), is commonly known as the Swedish method, and was improved by Bishop (3) and others.

Herein the varved clay foundation material of the New Liskeard embankment will be subjected to both total and effective stress analyses to ascertain the reasonable assumptions for the varved soil that failed when the embankment reached a height of 16.6 ft (5.7 m). The failure has previously been discussed by Lo and Stermac (10). At a distance of 426.5 ft (130 m) from the failure, the embankment foundation was instrumented; part of the construction performance below the instrumented area has been described by Stermac, Lo, and Barsvary (20), and the immediate or undrained performance has been analyzed and presented by Raymond (17). The pore pressure response of this instrumented area will be used in conjunction with tests described herein to perform the effective stress analysis.

SITE GEOLOGY

The sedimentary soils in the Timiskaming area are a product of postglacial deposition following the retreat of the Wisconsin ice sheet. Meltwater and subglacial rivers were prevented from draining through the Ottawa River basin by the relatively high lands in the North Bay-Mattawa region. Consequently, the water rose, forming glacial Lake Timiskaming, which occupied a basin somewhat larger than the present lake. The retreat of the glacier in the immediate area was rather rapid: Antevs (1) suggests 492 ft (150 m) per year. There was a temporary halt, however, when the face of the glacier

reached the highlands just north of the Cochrane area. During this period, because of the lack of adequate drainage, the lake increased immensely in size forming what Wilson (25) has named Lake Barlow. In the early stages of its development when Lake Timiskaming was relatively small and the discharge of sediments into it was relatively high, seasonal deposition resulted in thick varved sediments, particularly in the deeper parts of the basin. As the lake became larger and the front of the glacier moved away from the lake, the material became more dispersed, and the resulting varves were much thinner. Consequently, the varved sediments in this area display a much greater varve thickness in the lower region of the deposit than near the surface.

Using pollen counts, Terasmae and Hughes (21) suggested a possible time-temperature variation for the Timiskaming area that implies a possible readvance and retreat of the glacier in this region.

The area in which the bypass is situated lies on a relatively flat plane on the margin of the Lake Timiskaming basin. The clay deposit extends to a depth of about 147.6 ft (45 m) at the proposed site of the overpass and is at the surface at a point 1,968 ft (600 m) to the southwest.

Below the varved clay is about 0.98 ft (0.3 m) of dense sand and gravel resting on bedrock, the upper 0.9 ft of which was reported as fractured and weathered banded gray and white limestone. It is believed that the dense sand and upper fractured zone of bedrock serve as a drainage course for the area. Indeed the measured pore pressures prior to construction suggest a downward drainage throughout the deposit, the pore pressures being less than hydrostatic below the water table at 4.9 ft (1.5 m) below the surface.

SOIL PROPERTIES

Samples were taken with a commerical Shelby 2.75-in. (70-mm) diameter fixed piston sample tube from the centerline of the embankment at the instrumented section. The sample tubes were cut before the soil was extruded, and then the soil was trimmed to 1.5 in. ($37\frac{1}{2}$ mm) in diameter by 2.9 in. (75 mm) long. Several samples were initially consolidated to about their overburden pressure or three-quarters of their preconsolidation pressure, as recommended by Raymond, Townsend, and Lojkasek (18) and tested in undrained compression in a triaxial cell. Ideally they should be consolidated isotropically or anisotropically by using a lateral pressure $\frac{1}{2}$ to 1 time their field effective overburden, provided this does not exceed one-half to three-quarters of their preconsolidation pressures. This latter requirement permits the maintenance of the in situ grain structure of the soils, assuming good sampling. They were then reconsolidated at a cell pressure greater than their greatest failure stress and retested in undrained compression (stage 2). The second stage was repeated a third time. The failure index was defined as the axial stress difference/axial failure stress difference $[(\sigma_1 - \sigma_3)/(\sigma_1 - \sigma_3)_f]$; the failure index-strain results from the first stage are given in Table 1 along with the average values from all three stages. The consolidation pressures prior to failure and the failure stresses are given in Table 2.

The soil in the ground was believed fully saturated, and this was ensured in the laboratory tests by the use of a back pressure. Thus the pore pressure coefficient B = 1. The triaxial pore pressure characteristics can thus be characterized by recording the pore pressure coefficient A. This has been done (Table 3) for the triaxial stage 1 tests by using different values of failure index. Also recorded are the average values for all three stages. The stage 1 averages are slightly smaller than those from the second and third stages, probably because of the slight overconsolidation existing after the first stage consolidation. The average values from the second and third stages, however, may be seen to be remarkably close as might be expected from the testing of remolded normally consolidated clays (4). Thus stage testing should preferably not be used to obtain the pore pressure coefficient A; this coefficient should be based on the first stage results. Another difference that can be noticed from the average results is that the coefficient A is less variable for the stage 1 results than for the other two stages, which is in agreement with the reported work on sampling effects on Leda clay (18).

The consolidated undrained tests with pore pressure measurements allow effective stress Mohr circles to be drawn. The circles obtained from the two samples closest to the surface are shown in Figure 1. These results are interesting insofar as the circles obtained at higher pressures allow an evaluation of the unstructured ϕ' to be obtained (i.e., the value of ϕ' that results in $c' = 0$, which is a common result for normally consolidated remolded clays). These values of unstructured ϕ' are tabulated and given in Table 2. The low pressure circle indicates that $c' \neq 0$ at low confining pressure. Unfortunately when these tests were performed, little was known about the strength properties of cemented soils. Based on the work of Townsend, Sangrey, and Walker (24) and Raymond and coworkers (18), much more emphasis should have been put on obtaining good undisturbed soil samples and testing these samples at low confining pressure. Herein only the results available can be used, and thus the unstructured values of ϕ' will be used.

The values of ϕ' given in Table 2 are different with depth. Townsend et al. (23) have shown that some of this variation can be accounted for by composition in terms of finer and coarser grained layers of the varved specimens tested. By taking a conservative value of the results, which would correspond to a varved structure when the finer grained layers predominate, a value of $\phi' = 24$ deg was selected for the effective stress analysis reported herein.

A second set of trimmed samples was tested in unconfined compression, whereas a third set was more recently obtained with a Swedish piston sampler, modified so as to have rigid piston fixing rods and tested at the sampler diameter of 1.9 in. (50 mm), i.e., no trimming. The results from the third set are given in Table 3. In addition to unconfined compression tests this third set of samples was tested in the odometer to obtain the preconsolidation pressure of the soils. The failure strengths and preconsolidation pressures are shown in Figure 2 along with the typical in situ vane test results. The results shown in Figure 2 are from the instrumented section of the embankment. Figure 3 shows details of in situ vane tests along with the usual identification tests (i.e., plastic limit, in situ moisture content, bulk specific gravity, and liquid limit) from the failed area of the embankment some 426 ft (130 m) from the instrumented area. The strength results shown in Figures 2 and 3 are very similar and may be approximated below the desiccated crust by

$$c_u = 10.0 + 1.83\ z \quad kN/m^2 \tag{1}$$

where z is the depth below the surface. The crust may be seen to be about 9.8 ft (3 m) deep and the strength of the crust if projected to the surface results in a maximum surface value of 75 kN/m^2. Thus for the upper 9.8 ft the maximum strength measured is

$$c_u = 75 - 16.5\ z \quad kN/m^2 \tag{2}$$

INSTRUMENTATION AND PORE PRESSURE RESPONSE

The instrumentation used at the New Liskeard embankment site is shown in Figure 4. The instrumentation was placed 1 year prior to construction. Construction was completed rapidly with 18.7 ft (5.7 m) of fill being placed within 30 days. As mentioned earlier, some details of the overall performance are given by Stermac, Lo, and Barsvary (20), and details of the undrained performance are analyzed and presented by Raymond (17). The failure of the embankment has previously been analyzed by Lo and Stermac (10), who also gave survey details of the section that failed.

The pore pressure response measured in those piezometers that were still in working order below the toe is shown in Figure 5. The pore pressure may be seen to increase for some time after the end of construction. The exact reason for the post-construction increase in pore pressure is unknown, but contributing factors are probably undrained creep (Walker, 1969), stress redistribution during consolidation, and lateral drainage. Figure 6 shows the measured pore pressure plotted against depth at the end of embankment construction (30 days) and 30 days later (60 days). The latter time corresponds to the estimation made by Raymond (17) of the end of major undrained

Table 1. Percentage of strain for consolidated undrained tests on varved clay.

Sample Depth (m)	σ_c' (kN/m²)	$(\sigma_1 - \sigma_3)/(\sigma_1 - \sigma_3)_f$ ½	¾	⅞	15/16	1
1.52	36	0.65	1.75	2.80	3.70	5.37
4.57	27	0.32	0.77	1.17	1.40	2.69
7.63	61	0.20	0.70	1.30	1.90	3.37
10.6	115	0.22	0.48	1.08	1.44	3.00
13.7	130	0.12	0.50	1.10	1.75	4.36
16.8	162	0.16	0.48	0.90	1.20	2.45
19.8	170	0.16	0.43	1.02	1.60	3.17
22.9	237	0.20	0.47	0.77	1.06	2.21
25.9	280	0.27	0.44	0.65	0.89	2.52
29.0	480	0.06	0.24	0.42	0.58	1.38
35.0	305	0.25	0.45	0.66	0.87	2.15
38.1	416	0.28	0.48	0.76	1.06	2.63
41.2	447	0.24	0.40	0.65	0.90	1.70
Average stage 1		0.24	0.58	1.02	1.41	2.84
Average stage 2		0.17	0.45	0.87	1.43	3.06
Average stage 3		0.20	0.52	1.03	1.42	3.36

Table 2. Triaxial failure stresses (kN/m²).

Sample Depth (m)	Percentage of Finer Grained Layer	Stage 1 σ_c'	Stage 1 $(\sigma_1 - \sigma_3)_f$	Stage 2 σ_c'	Stage 2 $(\sigma_1 - \sigma_3)_f$	Stage 3 σ_c'	Stage 3 $(\sigma_1 - \sigma_3)_f$	ϕ' (c' = 0)
1.52	75	36	78	144	150	324	266	33.0
4.57	67	27	48	144	83	288	171	25.0
7.63	0	61	67	180	146	360	330	32.8
10.6	83	115	84	252	142	432	232	22.0
13.7	43	130	87	290	164	576	335	26.5
16.8	68	162	120	360	189	576	355	25.0
19.8	50	170	136	360	212	612	378	26.5
22.9	67	237	197	502	286	865	572	28.5
25.9	14	280	178	576	379	1,080	836	30.5
29.0	62	480	307	936	494			24.0
35.0		305	290					
38.1		416	264					
41.2		447	477					

Figure 1. Typical Mohr circles from triaxial stage tests.

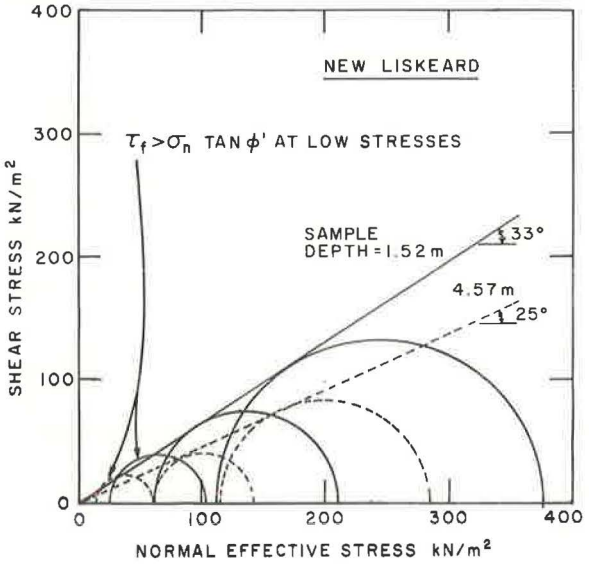

Table 3. Percentage of strain for unconfined compression tests from Swedish sampling.

Sample Depth (m)	$(\sigma_1 - \sigma_3)/(\sigma_1 - \sigma_3)_f$					$(\sigma_1 - \sigma_3)_f$ (kN/m²)
	½	¾	⅞	15/16	1	
3.8	0.52	0.98	1.45	1.78	2.50	39
4.0	0.54	1.20	1.75	2.10	3.00	28
5.8	0.40	0.72	0.98	1.16	1.67	41
6.0	0.44	0.90	1.24	1.46	2.10	47
6.3	1.85	3.10	4.35	5.20	7.20	46
7.8	3.01	5.54	7.35	8.45	9.75	83
8.0	1.27	2.30	3.25	4.0	5.12	49
8.5	1.50	2.40	3.40	4.30	6.40	48
9.8	0.48	0.80	1.11	1.34	1.80	55
10.0	2.40	3.23	3.95	4.54	5.84	49
10.3	0.63	1.00	1.32	1.40	2.40	54
12.0	0.60	1.00	1.32	1.65	2.50	62
12.3	0.80	1.30	1.80	2.10	3.10	70
13.0	0.55	0.90	1.10	1.22	2.00	85
13.3	0.50	0.88	1.06	1.20	2.00	90
15.3	0.37	0.59	0.73	0.83	1.06	89
17.3	1.38	2.10	2.63	3.02	4.13	75
18.0	0.70	1.70	3.03	3.74	4.80	64
21.3	0.66	1.16	1.83	2.35	3.13	47
23.3	0.80	1.90	2.68	3.01	3.48	55
25.3	0.49	0.77	1.03	1.23	1.49	50
27.3	0.65	1.11	1.69	2.22	3.43	58
29.3	0.56	0.82	1.01	1.21	1.68	50
Average	0.92	1.58	2.18	2.59	3.50	

Figure 2. Soil properties from borehole near instrumentation.

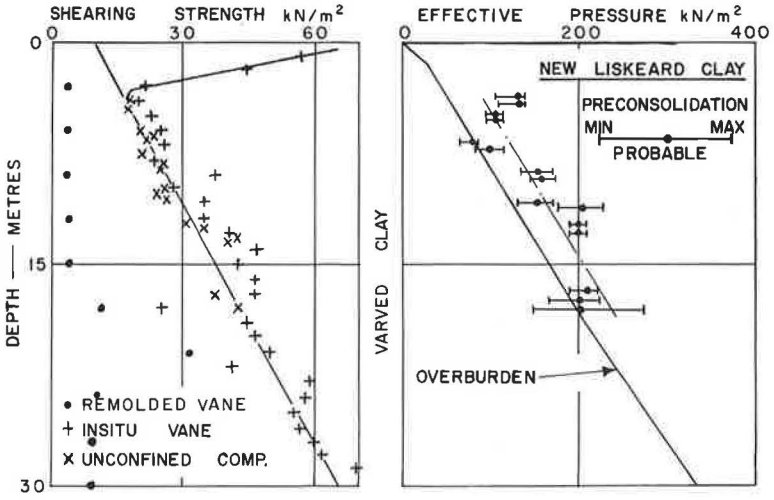

Figure 3. Soil properties from borehole near failed area (10).

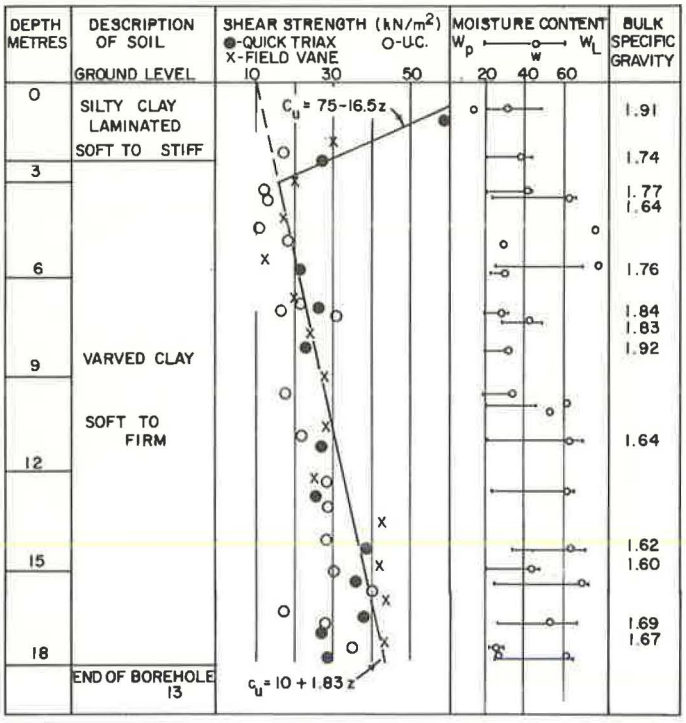

Figure 4. Details of instrumentation.

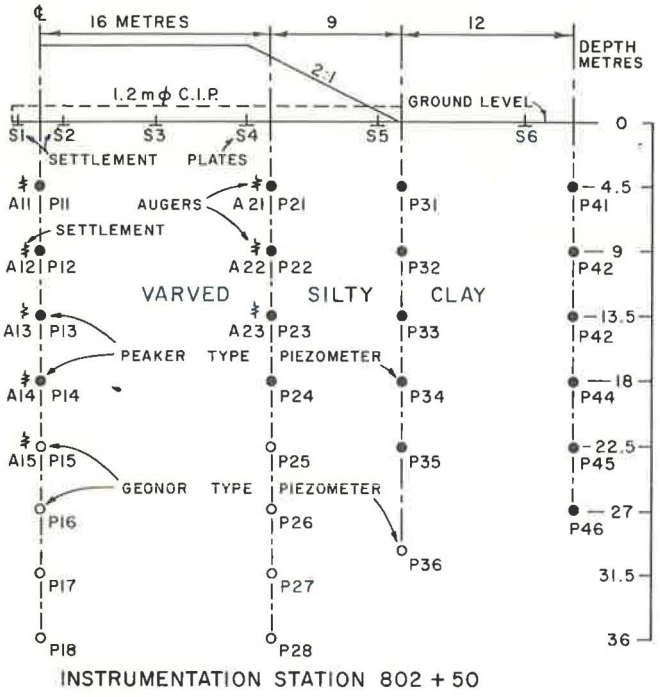

Figure 5. Measured excess pore pressures below toe.

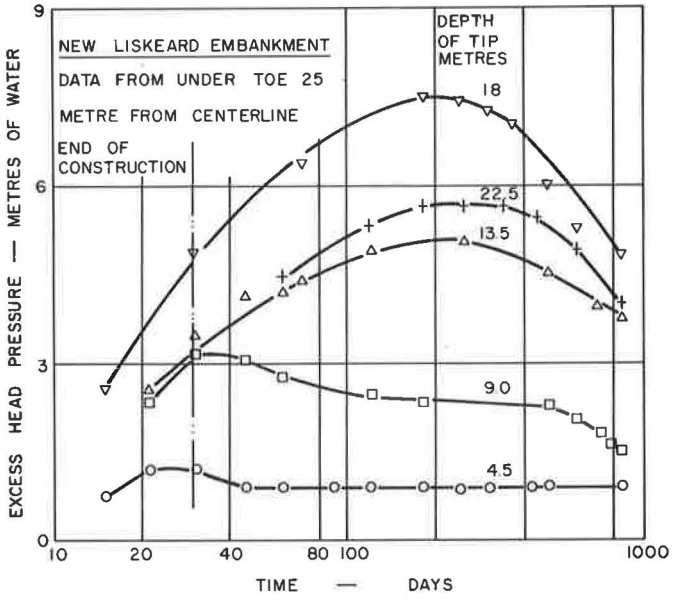

Figure 6. Excess pore pressures at and shortly after the end of construction.

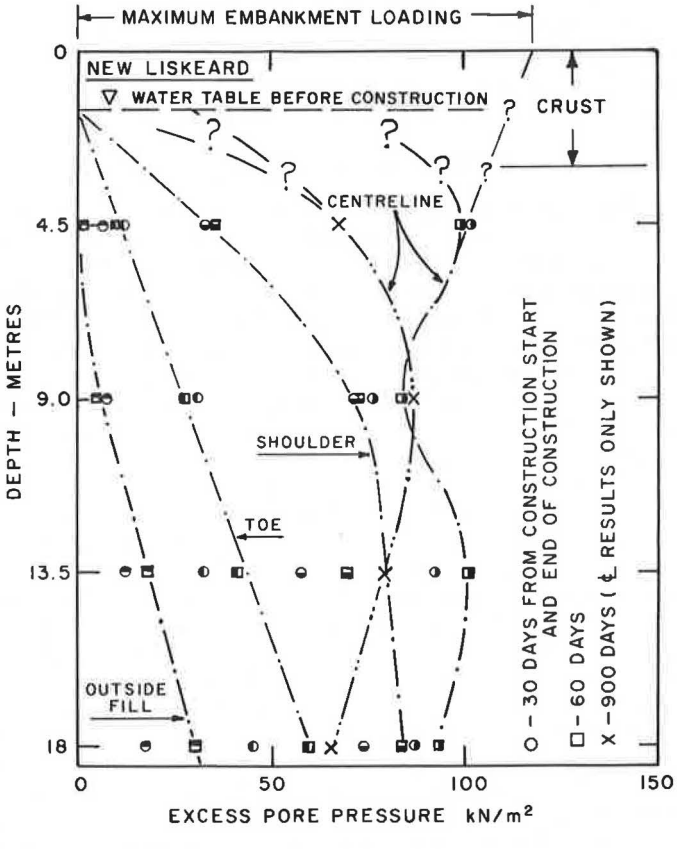

movements or movements occurring without loss of water from the soil at depth. Also shown are the pore pressures measured below the centerline at 900 days.

The pore pressures shown in Figure 6 with the exception of those below the centerline suggest that the drainage face near the surface corresponds approximately to the water table prior to construction (i.e., 1.5 m deep). The results below the centerline are inconclusive as regards the drainage face, and it may well be that the weight of the fill was large enough below the full height of the embankment to cause a large decrease in the permeability of the crust soil material. Thus the drainage face below the center of embankment may have moved upward to the surface of the foundation soil.

The measured pore pressure only gives the pore pressure at specific locations. To estimate the effective stress stability requires that the pore pressures on the slip circle be calculated. Raymond (17) used finite elements to obtain reasonable agreement (Fig. 7) between the measured pore pressures and the laboratory pore pressure coefficient A (assuming B = 1) by using the equation suggested by Skempton (19):

$$\Delta_u = \Delta\sigma_3 + A\,(\Delta\sigma_1 - \Delta\sigma_3) \qquad (3)$$

where $\Delta\sigma_1$ and $\Delta\sigma_3$ are the principal increases in total stress, and the value of A is obtained from laboratory tests at the same percentage of failure as given for the point under consideration from the finite element result. Obviously the use of finite elements to calculate the pore pressure in many practical jobs would be overly expensive and unwarranted. For this reason a similar approach was attempted by using the Boussinesq stress increases except that the coefficient A used was the failure value. These results are shown in Figure 8 where the Boussinesq stress distribution below the four locations is also shown. It may be seen that the estimated pore pressures using the failure coefficient A lead, in general, to predicted pore pressures slightly greater than those measured, and thus such an approach would lead to conservative effective stress stability factors of safety. Because of the simplicity of calculating the Boussinesq stress increase, this approach was adopted for the study reported herein.

TOTAL STRESS AND PARTIAL TOTAL STRESS ANALYSIS

The method of analysis used was that described by Bishop (3) modified when $\phi \neq 0$ as required. These modifications are given in the Appendix. No strength was assigned to the fill; thus, when $\phi = 0$ in the foundation material, Bishop's method of analysis will correspond to the Swedish slip circle or method of slices. Two analyses were done. The first used 20 slices of equal width, and the second used 20 slices of variable width with equal depth spacings of the slices. These two methods gave factors of safety within 5 percent of each other; the equal width method generally gave slightly lower factors of safety. The analysis was programmed for a computer so that a large number of slip circles of various radii and slip circle center coordinates could be tried until the minimum safety factor was found.

In the analysis of low, wide embankments built of granular material, it seems reasonable to neglect the resistance to rotational failure contributed by the embankment. In a slip circle analysis the failure surface is steepest in the fill, and thus the frictional resistance will tend to be smallest. Lo and Stermac (10), for example, in their analysis of the New Liskeard embankment concluded that the fill strength contributed 6 to 10 percent of the value of the factor of safety. Jakobson (9) uses the assumption of no fill strength in discussing the design of embankments on soft clays. In addition it must be remembered that, in general, the fill will be constructed of a soil different from the foundation soil. The stress-strain characteristics of these two soils may be expected to be different. Thus their peak strengths will not, in general, be mobilized simultaneously. It therefore seems reasonable to neglect the strength of the fill. This assumption is confirmed by the actual failure through the embankment where the failure was vertical through the fill. Typical photographs are shown by Lo and Stermac (10).

Figure 9 shows the results of the computations assuming $\phi = 0$ below the crust. Above the crust a number of different assumptions were taken. The results obtained with the most realistic of these assumptions are shown in Figure 9. First, three complete total stress analyses were performed. These three assumptions were

Figure 7. Comparison of excess pore pressures measured with those predicted from finite element analysis.

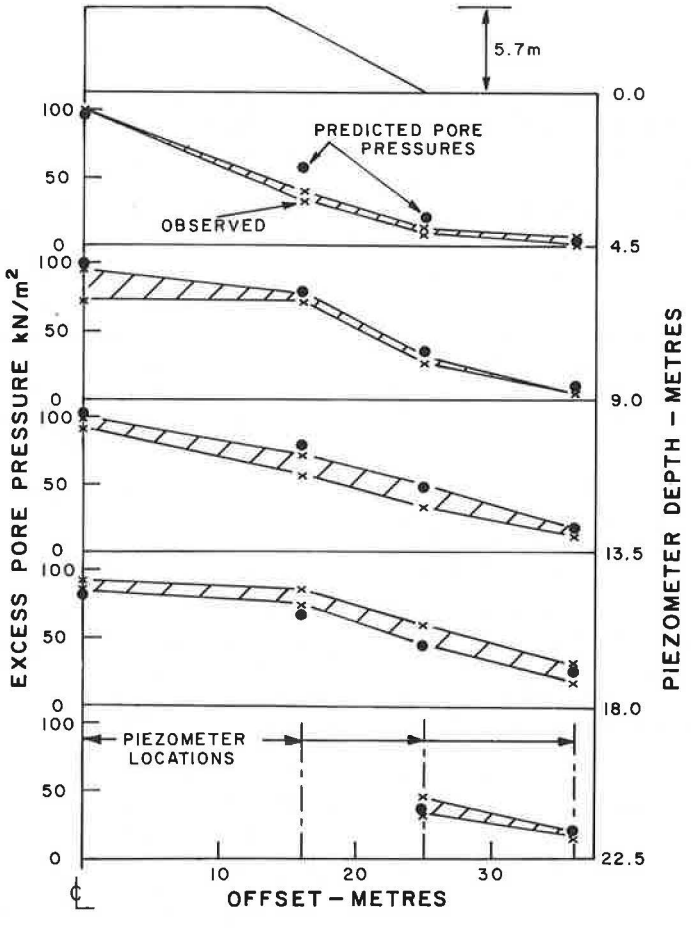

Figure 8. Comparison of excess pore pressures measured with those predicted from Boussinesq stress distribution.

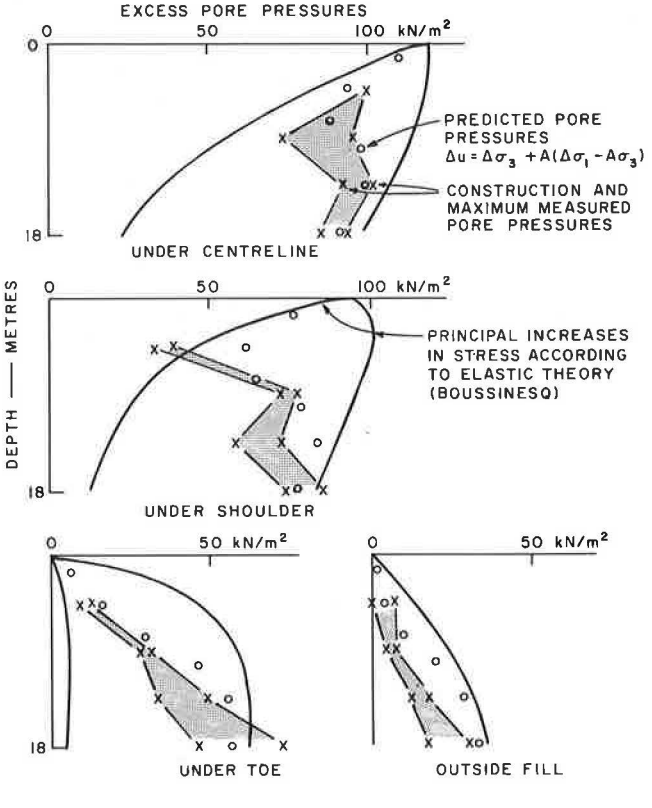

1. That the soil had no crust so that the soil strength equation below the crust was valid in the crust, $c_u = 10.0 + 1.83\ z$ kN/m^2;
2. That the soil had a constant crust strength, $c_u = 15.5$ kN/m^2 to a depth of 9.8 ft (3 m), which is the soil strength at 9.8 ft (i.e., the bottom of the crust); and
3. That the full measured crust strength was $c_u = 75 - 16.5\ z$ kN/m^2 to a depth of 9.8 ft (3 m) and $c_u = 10 + 1.83\ z$ kN/m^2 below 9.8 ft.

At 9.8 ft (3 m) these equations give the same strength of 15.5 kN/m^2. These three methods result in factors of safety of 0.88, 0.93, and 1.30 respectively.

Second, some partial total stress analyses were calculated. The same shearing strength equation was assumed below the 9.8-ft (3-m) thick crust while an effective stress analysis was used for the crust. Two results are shown in Figure 9. In both cases shown $c' = 0$, $\phi' = 24$, bulk specific gravity = 2.0, and the water table was taken as 4.9 ft (1.5 m) below the surface. The other assumptions were (for the 9.8-ft crust)

1. That excess pore water pressures were given by $\Delta_u = \Delta\sigma_3 + A_f\ (\Delta\sigma_1 - \Delta\sigma_3)$ where the stress distribution was given by Boussinesq and A_f was interpolated from Table 3—0 at the surface, 0.15 at 4.9 ft (1.5 m), and 0.21 at 9.8 ft (3 m); and
2. That excess pore pressures completely dissipated.

These two assumptions resulted in factors of safety of 0.96 and 1.17, but the assumptions on excess pore pressure in the crust gave a critical failure circle closest to that actually surveyed. These are all shown in Figure 9. The effect of moving the water table to the surface reduced these factors of safety to 0.72 and 1.10. These last sets of results indicate quite a substantial effect of the assumed position of the water table in an effective stress analysis.

The fact that treating the crust as an effective stress analysis gives factors of safety less than those obtained by using the full undrained strength in the crust is in agreement with observations by Raymond (16, 17). Raymond found that drained tests on the crust soil conducted at confining pressures equal to the effective overburden from the site of an embankment at Kars, Ontario, resulted in strengths considerably less than unconfined compression or in situ vane strengths. Indeed the drained strengths were less at confining pressures equal to the effective overburden plus the overburden due to the first stage fill height of 19.7 ft (6 m) than the conservative selected undrained strength of the crust soil.

The use of a total stress analysis results in a critical circle whose center lies above the center of the slope. As a change is made to effective stress analysis the critical circle center moves toward the toe and to a point above the $^1/_3$ rad slope height (Fig. 9). In the analysis performed when a partial total stress analysis was undertaken, two or more circle centers gave the same factors of safety. A second point to be noted is the shallowness of the failure circles except when the full crust strength is assumed. The depth of these circles is generally less than 19.7 ft (6 m).

EFFECTIVE STRESS ANALYSIS

The effective stress analyses were carried out by using the method described by Bishop (3) modified as in the Appendix and used in the partial total stress analyses. No strength was assigned to the fill for reasons previously presented. Several possible assumptions were investigated. Both equal slice and variable slice widths were used. Again the difference in results was small. Three results for equal slice width are shown in Figure 10. In each case $c' = 0$, $\phi' = 24$, bulk specific gravity = 2.0, and the water table was taken as 4.9 ft (1.5 m) below the surface. The pore pressure coefficient A_f was assumed to vary as given in Table 4 to a depth of 34.9 ft (13.7 m) at which point A_f was taken as 0.9 and constant with depth. The three additional sets of assumptions were

1. That excess pore water pressures are given by $\Delta_u = \Delta\sigma_3 + A_f\ (\Delta\sigma_1 - \Delta\sigma_3)$, where the stress distribution was given by Boussinesq;
2. That excess pore water pressure was as above but completely dissipated above water table; and
3. That excess pore water pressure completely dissipated in whole mass.

These assumptions resulted in factors of safety of 1.17, 1.58, and 2.39 respectively. Raising the water table to the surface reduces the factors of safety to 0.72, 1.21, and 1.96. This again shows the importance of exactly locating the water table for effective stress analysis.

The location of the critical circle by using the full excess pore water pressures is given by a very shallow failure circle that is unacceptable from a practical point of view. The factor of safety of 1.17 is, however, the most acceptable of effective stress values for the analyses with the water table at 4.9-ft (1.5-m) depth. The large differences in the calculated factors of safety indicate that the use of the effective stress method is very much dependent on making rather precise, realistic assumptions because small errors will result in large errors in the factor of safety. It also suggests that stability could be improved with relatively shallow sand drains.

It may be seen from Figure 10 that the use of an effective stress analysis results in critical circles for this foundation with centers above the $\frac{1}{3}$ rad slope height. The depth of the circles is also less than 19.7 ft (6 m). These results would seem to be reasonable indicators of where the instrumentation should be concentrated at this site had the observational method (14) been used for controlling construction to the fill height of 19.7 ft (6 m).

FINITE ELEMENT TOTAL STRESS ANALYSIS

The method used herein to predict the overstressed areas below the New Liskeard embankment was finite element analysis. A full description of the procedure is given by Raymond (17) and is summarized here. The failure index-strain relationship was assumed uniform throughout the deposit. The average values obtained from the consolidated undrained tests given at the bottom of Table 1 were taken to be the design values. After failure the shearing strength was assumed constant. It is well known that the shearing strengths from consolidated undrained tests vary with the consolidation pressure; thus the tests cannot be used to estimate the in situ shearing strength. In a weak deposit such as that at New Liskeard it is common to use in situ vane shear tests supported by unconfined compression tests to obtain the in situ strengths. This procedure was followed for the analysis. Poisson's ratio was taken as 0.49 inasmuch as the finite element method does not permit the use of 0.5.

Using coarse finite elements or small elements had far less effect on the results than the material properties assumed for the elements. Figure 11 shows the failed elements using the assumption

$$c_u = 10 + 1.83\ z \quad kN/m^2$$

throughout the deposit and a multilinear stress-strain relationship. It may be seen that failure has occurred in sufficient elements that the finite elements will continue to yield. Thus using the above equation as valid for the strength throughout the whole deposit including the top 9.8 ft (3 m) results in a failure of the embankment foundation. The similarity in the computed failed mass with the observed failure is very encouraging regarding further development of the finite element method.

When a full crust strength and the same multilinear stress-strain derivation were assumed, no failed elements resulted from a finite element analysis. On the other hand assuming a full crust strength and a bilinear material based on an initial modulus using the average strain at one-half failure (the strains at a failure index of $\frac{1}{2}$ given in Table 1) and a zero second or final modulus resulted in a large number of failed elements occurring below the central portion of the fill (Fig. 12). Although the failed elements shown in Figure 12 are coarse, the same pattern was obtained with elements one-third the vertical linear dimension. Figures 11 and 12 confirm the finding regarding the major effect of the assumed stress-strain relationship. In addition a multilinear analysis was performed by using a constant crust strength of 15.5 kN/m^2, which resulted in a failure pattern similar to that shown in Figure 11 except that the failed area was not so extensive. This is shown in Figure 13. The analysis indicates that the failed elements are just about to spread to the surface at the toe, which indicates a factor of safety

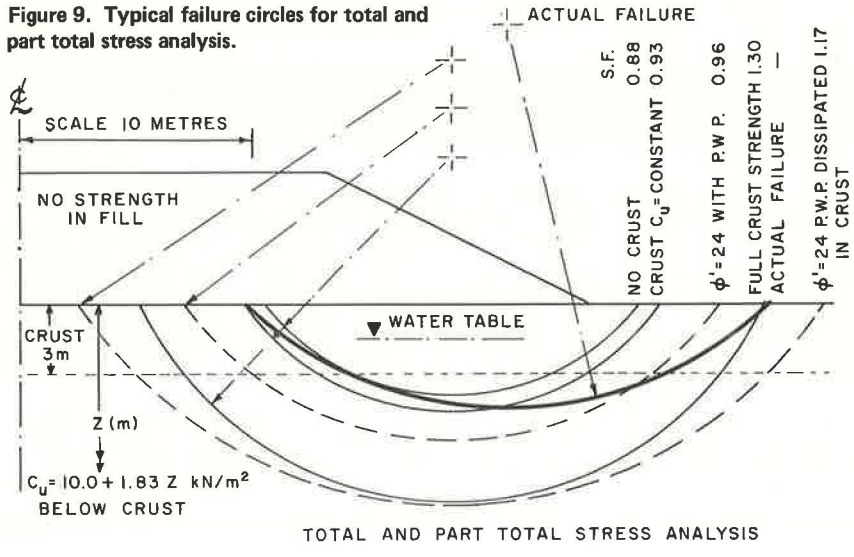

Figure 9. Typical failure circles for total and part total stress analysis.

Table 4. Pore pressure coefficients for New Liskeard varved clay.

Sample Depth (m)	σ_o' (kN/m²)	$(\sigma_1 - \sigma_3)/(\sigma_1 - \sigma_3)_f$ ½	¾	⅞	15/16	1
1.52	36	0.61	0.41	0.25	0.18	0.15
4.57	27	0.28	0.32	0.31	0.29	0.27
7.63	61	0.45	0.49	0.49	0.48	0.47
10.6	115	0.30	0.46	0.57	0.63	0.76
13.7	130	0.59	0.77	0.83	0.85	0.99
16.8	162	0.76	0.76	0.78	0.80	0.90
19.8	170	0.55	0.62	0.73	0.77	0.83
22.9	237	0.55	0.60	0.64	0.66	0.77
25.9	280	0.63	0.65	0.74	0.84	1.06
29.0	480	0.44	0.69	0.73	0.75	0.80
35.0	305	0.58	0.58	0.59	0.60	0.75
38.1	416	0.51	0.51	0.66	0.74	0.91
41.2	447	0.74	0.74	0.87	0.92	1.08
Average stage 1		0.54	0.58	0.63	0.65	0.75
Average stage 2		0.56	0.64	0.71	0.78	0.94
Average stage 3		0.55	0.65	0.71	0.77	0.88

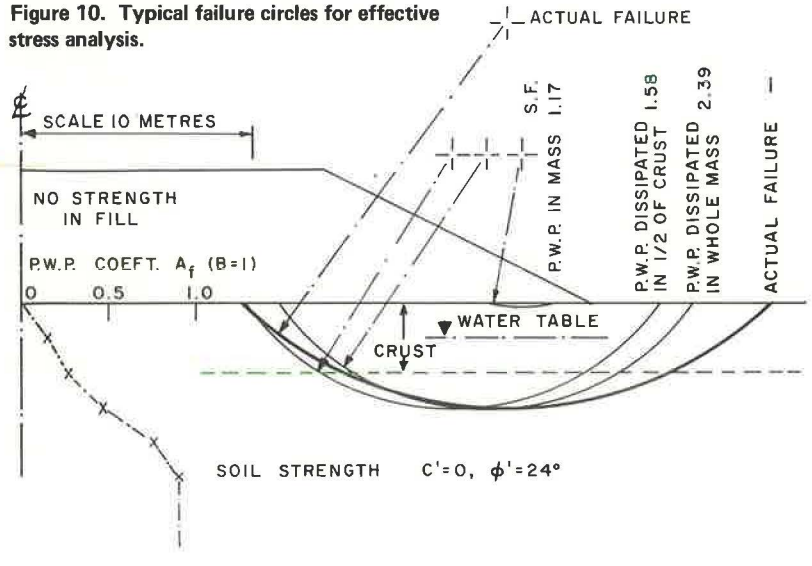

Figure 10. Typical failure circles for effective stress analysis.

Figure 11. Failed elements from finite element analysis with no increased strength in crust and multilinear stress-strain soil properties.

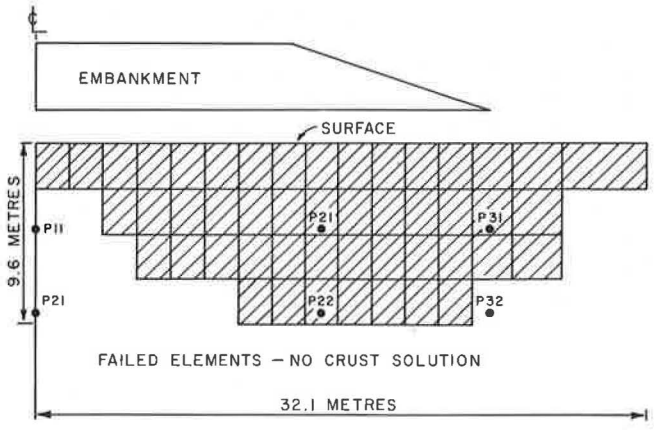

Figure 12. Failed elements from finite element analysis with full crust strength and bilinear stress-strain soil properties.

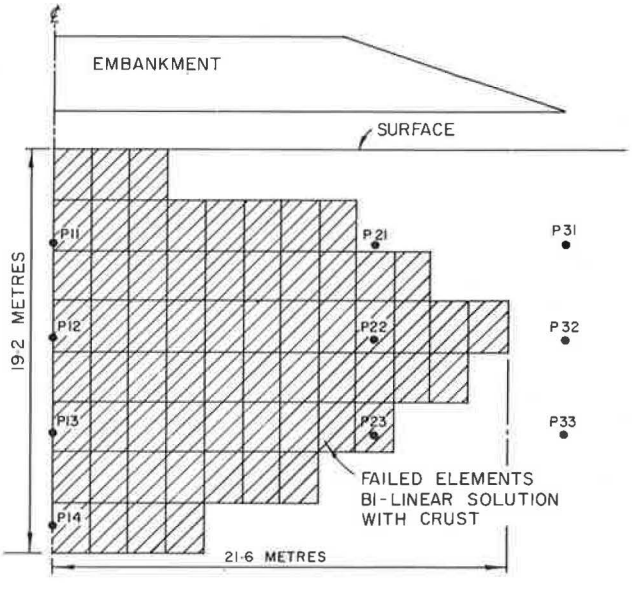

Figure 13. Failed elements from finite element analysis with constant crust strength and multilinear stress-strain properties.

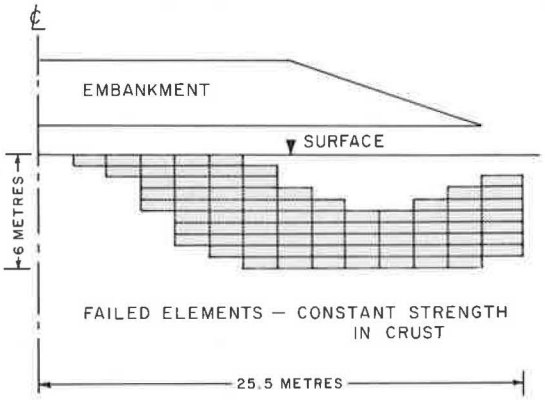

close to one. The similarity between the computed failed mass using multilinear analysis and observed failure (Figs. 11 and 13) is very encouraging regarding further development of the finite element method. Obviously the major question is still what assumptions are to be made regarding the design strength of the crust. The importance of the multilinear approach has, of course, already been emphasized.

The finite element method can in some cases be most valuable. This is demonstrated by Hollingshead and Raymond (8), who analyzed the performance of an embankment foundation involving peat and lake marl overlying soft clay. The peat and lake marl consolidated quickly with the placement of berms, whereas the central fill caused the underlying clay to squeeze laterally outward causing large settlements without any observable slip circle reaching the surface.

CONCLUSIONS

The performance of an instrumented section of the New Liskeard embankment along with laboratory and in situ tests has been used to analyze the failure of a similar height of the same embankment situated (130 m) away that failed. For this embankment foundation tentative conclusions may be drawn.

1. The near failure excess pore pressures in the foundation material may be calculated with sufficient accuracy for practical purposes from a Boussinesq stress distribution increase and Skempton's pore pressure equation (19) by using failure pore pressure coefficients

$$\Delta u = \Delta\sigma_3 + A_f\,(\Delta\sigma_1 - \Delta\sigma_3)$$

the pore pressure coefficient A_f being obtained from samples that are laboratory-consolidated isotropically at or just below (between $^1/_2$ and 1 time) their overburden pressure and less than one-half to three-quarters their preconsolidation pressure.

2. The major problem in using undrained test results in a total stress analysis is the assignment of soil strengths to the crust material. The crust material generally has an unconsolidated undrained strength greater than its drained strength. The most realistic factor of safety was obtained by using effective stress analysis with estimated pore pressures in the crust material and undrained total stress analysis below the crust. Any use of effective stress analysis was, however, found to be very sensitive to the position of the preconstruction water table. Thus the preconstruction water table should be very carefully determined where stage construction techniques are to be used.

3. Both the actual failure and the estimated failure circles were found to be very shallow, extending generally to a depth less than 19.7 ft (6 m). They also extended to their deepest position below the $^1/_3$ slope height. Thus, for controlling construction, the instrumentation for a fill height of 19.7 ft (6 m) should be located below and to either side of the $^1/_3$ slope height to a depth of at least 19.7 ft.

4. The use of the most realistic effective stress analysis parameters (i.e., with undrained excess pore pressures throughout the mass) resulted in a very shallow unrealistic slip circle although the factor of safety was only slightly too large (1.17). In view of the shallowness of the failure circles it is believed that improvement to the stability at this site could be obtained with relatively shallow sand drains.

5. The finite element analysis was found to be useful in predicting the failed area by using a pseudo total stress analysis, provided multilinear stress-strain properties were used. If bilinear soil properties were used, the yield zone became unrealistic in terms of the observed failure.

ACKNOWLEDGMENT

The instrumentation was installed as a research program on the consolidation properties of varved clays. The program was conducted jointly by the Ministry of Transportation and Communications of Ontario and Queen's University with financial aid to Queen's University from the MTCO. Additional financial assistance was received from the National Research Council of Canada.

Gratefully acknowledged is the cooperation of a large number of individuals, in particular, D. L. Townsend, J. A. Cruickshank, and D. E. Hilts, formerly of Queen's University, and A. G. Stermac of the Ministry of Transportation and Communications of Ontario.

REFERENCES

1. Antevs, E. Retreat of the Last Ice Sheet in Eastern Canada. Geological Survey of Canada, Memo. 146, 1925.
2. Barron, R. A. Discussion. Geotechnique, Vol. 16, No. 4, 1964, pp. 360-361.
3. Bishop, A. W. The Use of the Slip Circle in the Stability Analysis of Slopes. Geotechnique, Vol. 5, No. 1, 1955, pp. 7-17.
4. Bishop, A. W., and Henkel, D. J. The Measurement of Soil Properties in the Triaxial Test, 2nd Ed. Edward Arnold, 1962, p. 227.
5. Felenius, W. Erdstatische Berechnungen mit Reibung and Kohaesion. Ernst, Berlin, 1927.
6. Felenius, W. Calculation of the Stability of Earth Dams. Trans. Second Internat. Congress on Large Dams, Vol. 1, 1936, p. 329.
7. Gibson, R. E. Discussion. Jour. Institution of Civil Engineers, Vol. 34, 1950, pp. 382-383.
8. Hollingshead, G. W., and Raymond, G. P. Prediction of Undrained Movements Caused by Embankments on Muskeg. Canadian Geotechnical Jour., Vol. 8, No. 1, 1971, pp. 23-35.
9. Jakobson, B. The Design of Embankments on Soft Clays. Geotechnique, Vol. 1, No. 2, 1948, pp. 80-90.
10. Lo, K. Y., and Stermac, A. G. Failure of an Embankment Founded on a Varved Clay. Canadian Geotechnical Jour., Vol. 2, No. 3, 1965, pp. 234-253.
11. Nakase, A. Contribution to the Bearing Capacity of Soil Stratum. Rept. of Port and Harbour Technical Research Institute, Japan, No. 4, 1963, p. 34.
12. Nakase, A. Stability of Low Embankments on Cohesive Soil Stratum. Soils and Foundations, Vol. 10, No. 4, 1970, pp. 39-64.
13. Odenstad, S. Ground Bearing Pressure and Supporting Banks in Cohesive Soil. Jour. Vag-och, Vattenbyggaren, Stockholm, Vol. 2, 1960, pp. 60-62. (In Swedish.)
14. Peck, R. B. Advantages and Limitations of the Observational Method in Applied Soil Mechanics. Geotechnique, Vol. 19, No. 2, 1969, pp. 171-187.
15. Raymond, G. P. The Bearing Capacity of Large Footings and Embankments on Clays. Geotechnique, Vol. 17, No. 1, 1967, pp. 1-10.
16. Raymond, G. P. The Kars (Ontario) Embankment Foundation. ASCE Specialty Conf. on Earth and Earth Supported Structures, Purdue Univ., Vol. 1, 1972, pp. 319-340.
17. Raymond, G. P. Prediction of Undrained Deformations and Pore Pressures in Weak Clay Under Two Embankments. Geotechnique, Vol. 22, No. 3, 1972, pp. 381-401.
18. Raymond, G. P., Townsend, D. L., and Lojkasek, M. J. The Effect of Sampling on the Undrained Soil Properties of a Leda Soil. Canadian Geotechnical Jour., Vol. 8, No. 4, 1971, pp. 546-557.
19. Skempton, A. W. The Pore Pressure Coefficients A and B. Geotechnique, Vol. 4, No. 4, 1954, pp. 143-147.
20. Stermac, A. G., Lo, K. Y., and Barsvary, A. K. The Performance of an Embankment on a Deep Deposit of Varved Clay. Canadian Geotechnical Jour., Vol. 6, No. 1, 1969, pp. 45-60.
21. Terasmae, J., and Hughes, O. L. Glacial Retreat in the North Bay Area, Ontario. Science, Vol. 131, No. 3411, May 13, 1960, pp. 1444-1446.
22. Terzaghi, K. Theoretical Soil Mechanics. John Wiley, New York, 1943, p. 510.
23. Townsend, D. L., Hughes, G. T., and Cruickshank, J. A. The Effect of Pore Pressures on the Undrained Strength of a Varved Clay. Proc. 6th Internat. Conf. on Soil Mechanics and Foundation Engineering, Montreal, Vol. 1, 1965, pp. 385-389.

24. Townsend, D. L., Sangrey, D. A., and Walker, L. K. The Brittle Behaviour of Naturally Cemented Soils. Proc. 7th. Internat. Conf. on Soil Mechanics and Foundation Engineering, Mexico, Vol. 1, 1969, pp. 411-417.
25. Wilson, M. E. Timiskaming County, Quebec. Geological Survey of Canada. Memo. 103, 1918, pp. 141-145.

APPENDIX

APPLICATION OF BISHOP'S METHOD

Bishop (3) developed his method of stability of slopes based on the method of slices. The forces assumed by Bishop on a typical slice are shown in Figure 14, which also shows the definition of the symbols used.

The normal effective stress on the failure surface is

$$\sigma_n = \frac{P}{\ell} = \frac{P'}{\ell} + u$$

The shearing stress mobilized is given by

$$s = \frac{1}{F}\left[c' + \left(\frac{P}{\ell} - u\right)\tan\phi'\right]$$

[Barron (2) has shown that this is not strictly correct.] Taking moments about the center of the failure circle gives

$$\Sigma\, Wx = \Sigma\, s\ell R$$

Resolving forces vertically on slice and substituting in the above equation result in [see Bishop (3) for derivation]

$$F = \frac{1}{\Sigma W \times \sin\alpha}\,\Sigma\left[c' \times b + (W - u \times b + X_n - X_{n+1})\tan\phi'\right]\frac{\sec\alpha}{1 + \dfrac{\tan\phi' \times \tan\alpha}{F}}$$

Figure 14. Slice forces assumed for Bishop (3) analysis.

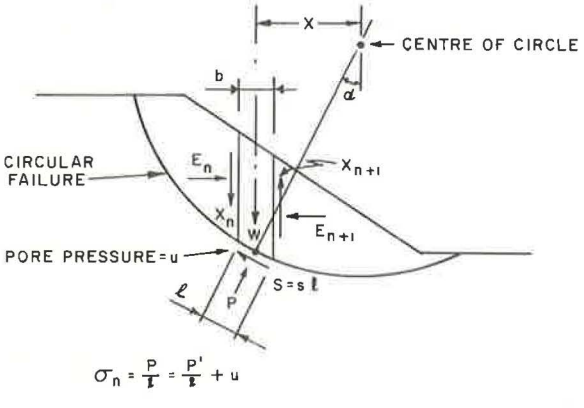

Bishop suggested that for slopes little loss of accuracy is obtained by assuming

$$X_n - X_{n+1} = 0$$

This simplification was assumed for the calculations reported herein. With this simplification, the normal effective force P' may be shown to be

$$P' = \frac{W - b\left(u + \frac{c'}{F}\tan\alpha\right)}{\cos\alpha\left(1 + \frac{\tan\phi'\tan\alpha}{F}\right)}$$

It is unlikely that either P' or $\left(1 + \frac{\tan\phi'\tan\alpha}{F}\right)$ can be negative. In fact when the stability of the New Liskeard embankment foundation was calculated, negative values of these terms did occur. Under such conditions the Bishop analysis was modified by making those terms that were negative in the summation equal to $\frac{b \times c'}{\cos\alpha}$.

In practice piezometers are often used to control construction. Under such conditions it is more desirable to calculate the ratio U_r of excess pore pressures required to obtain the design factor of safety u_f to the predicted excess pore pressures u_p. Bishop's equation can then be rewritten as

$$U_r = \frac{u_f}{u_p} = \frac{\Sigma\left[c' \times b + (W - u_o \times b)\tan\phi'\right]\frac{F \times \sec\alpha}{F + \tan\phi' \times \tan\alpha} - \Sigma F \times W \times \sin\alpha}{\Sigma u_p \times b \times \frac{F \times \tan\phi' \times \sec\alpha}{F + \tan\phi' \times \tan\alpha}}$$

where

u_o = initial water pressure due to the water table,
u_f = excess pore pressure required to reduce the stability to a factor of safety F, and
u_p = predicted excess pore pressure.

Values of U_r may be obtained for various values of F. Thus u_f may be obtained from U_r and u_p. The resident engineers can then be instructed to stop construction when any piezometer registers a preselected value of u_f for that piezometer. If U_r is less than or close to 1, controlled or stage construction must, obviously, be employed. Interestingly $u_f + u_o$ will be independent of the initial water table assumed (other terms being constant).